61-istam-sm-fp-537

Proceedings of 61st Congress of ISTAM (http://istam.iitkgp.ac.in)
Held at: VITU - Vellore, India, Dec. 11-14, 2016 (http://www.vit.ac.in/)

Nonlinear hybrid vibration absorber by time delay acceleration feedback

S Mohanty* and S K Dwivedy

Department of Mechanical Engineering, Indian Institute of Technology Guwahati, India 781039

Abstract

In the present work, analysis of a nonlinear time delayed hybrid vibration absorber (HVA) attached to a nonlinear single degree of freedom spring-mass-damper primary system is carried out. The primary system is subjected to harmonic and parametric excitation. It is proposed to reduce the vibration of both the primary and the absorber systems by attaching a lead zirconate titanate (PZT) stack actuator connected in series with a spring in absorber configuration which act as a hybrid vibration absorber (HVA). Due to the external excitation on the primary mass strain is developed in the PZT sensor, which produces voltage and this voltage converted to a counter acting force by the PZT actuator to supress the vibration of the primary system. The analysis is carried out by considering time delay acceleration feedback of the primary system. Harmonic balance method (HBM) is used to obtain the approximate solution of the system for primary resonance condition.

Keywords: DVA, PZT, HBM

1. Introduction

Dynamic vibration absorber (DVA) consists of spring mass damper system attached to host vibrating structure to suppress its vibration [1]. Various optimization methods such as H_2 optimization, H_∞ optimization, LQR method, genetic algorithm etc. are developed for attenuating vibration of the primary system and absorber [2]. To make the structure lighter and effective for broad band excitation various design of DVAs and smart materials are used [3, 4]. However nonlinearity with time delayed acceleration feedback control strategy is not explored more. In the proposed model a PZT actuator is connected in series with a spring by which one can use higher order stiffness value for the spring in series to produce more controlling force without any external voltage applied to the actuator.

2. Modelling of a nonlinear hybrid vibration absorber

A single degree of freedom primary system to which an active dynamic vibration absorber is placed is shown in Fig.1. Here m_i, c_i and k_i denotes mass, damping and stiffness of the primary system

*Corresponding author
E-mail address: siba.mech@gmail.com

Proceedings of 61st Congress of ISTAM (http://istam.iitkgp.ac.in)
Held at: VITU - Vellore, India, Dec. 11-14, 2016 (http://www.vit.ac.in/)

and the DVA respectively for $i=1,2$, k_3 denotes the stiffness of the absorber connected in series with PZT actuator having stiffness k_P^E. The terms k_{12}, k_{13}, k_{21} and k_{23} denote quadratic and cubic nonlinear stiffness in the primary system and absorber, respectively. The harmonic force of $F_{11}\cos(\Omega_{11}t)$ and a parametric excitation force of $x_1 F_{21}\cos(\Omega_{21}t)$ are acting on the primary system as shown in the Fig.1 (a). Due to these excitation forces strain is developed in the PZT sensor attached to the primary system. The displacement produced in the sensor is converted to voltage and through this voltage the PZT actuator produces a counteracting force on the primary system by providing acceleration feedback to the primary system. The block diagram of the acceleration feedback on the primary system $\ddot{x}_1$ with control gain k_c is shown in Fig. 1 (b). The mathematical model of the system is described by two ordinary coupled differential equations of motion as given in Eq. (1) and (2).

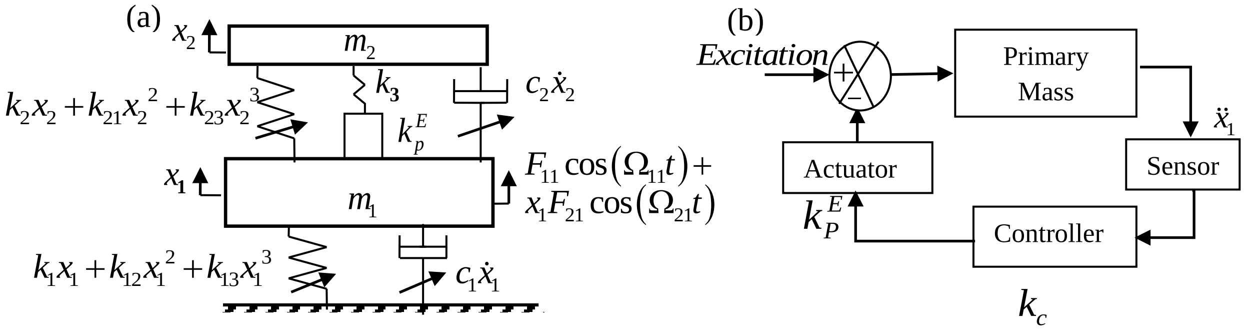

Fig.1 Piezoelectric stack actuator based nonlinear hybrid vibration absorber (b) Block diagram with acceleration feedback of primary system.

$$m_1\ddot{x}_1+k_1x_1+k_{12}x_1^2+k_{13}x_1^3+k_2(x_1-x_2)+k_{21}(x_1-x_2)^2+k_{23}(x_1-x_2)^3+c_1\dot{x}_1+c_2(\dot{x}_1-\dot{x}_2)$$
$$=F_{11}\cos(\Omega_{11}t)+x_1F_{21}\cos(\Omega_{21}t)-F_c \quad (1)$$

$$m_2\ddot{x}_2+k_2(x_2-x_1)+k_{21}(x_2-x_1)^2+k_{23}(x_2-x_1)^3+c_2(\dot{x}_2-\dot{x}_1)=F_c \quad (2)$$

Force developed by the actuator and spring in series can be written as $F_c=k_r(x_1+\delta_0-x_2)$ where $k_r=(k_3k_p^E)/(k_3+k_p^E)$ is the equivalent stiffness of the actuator and δ_0 is nominal displacement of the actuator at the junction of primary mass and actuator, which can be written as $\delta_0=nd_{33}V$. Considering the effect of time delay in the acceleration feedback of primary system i.e. $V=k_c(\ddot{x}_1-\ddot{x}_{1d})$ and substituting the value of V in F_c, the modified value of can be written as

$$F_c=k_r\left((x_1-x_2)-(x_{d1}-x_{d2})+nd_{33}k_c(\ddot{x}_1-\ddot{x}_{d1})\right) \quad (3)$$

Assuming $\omega_1 = \sqrt{k_1/m_1}$ and non-dimensional time $\tau = \omega_1 t$, the Eq. (1) and (2) can be written as

$$\ddot{x}_1 + \omega_{n1}{}^2 x_1 + (\alpha_{1c} + \alpha_{2c}) x_1 + h_{1c}\dot{x}_1 = \alpha_{2c}(x_{d1} - x_{d2}) + (\alpha_{1c} + \alpha_{2c}) x_2 - \alpha_{11c} x_1{}^2 - \alpha_{13c} x_1{}^3$$
$$-\alpha_{21c}(x_1 - x_2)^2 - \alpha_{23c}(x_1 - x_2)^3 + h_{2c}\dot{x}_2 + F_1\cos(\Omega_i\tau) + x_1F_3\cos(\Omega_3\tau) - F_{c1}(\ddot{x}_1 - \ddot{x}_{d1}) \quad (4)$$

$$\ddot{x}_2 + \omega_2{}^2 x_2 + \mu\alpha_{2c}x_2 - \mu(\alpha_{1c} + \alpha_{2c}) x_1 + \mu\alpha_{2c}(x_{d1} - x_{d2}) + \mu\alpha_{21c}(x_2 - x_1)^2 + \mu\alpha_{23c}(x_2 - x_1)^3$$
$$+\mu h_{2c}(\dot{x}_2 - \dot{x}_1) = \mu F_{c1}(\ddot{x}_1 - \ddot{x}_{d1}) \quad (5)$$

where

$$\omega_{n1} = 1, \mu = \frac{m_1}{m_2}, \omega_2 = \sqrt{\mu\frac{k_2}{k_1}}, \alpha_{1c} = \frac{k_2}{k_1}, \alpha_{2c} = \frac{k_r}{k_1}, h_{1c} = \left(\frac{c_1 + c_2}{m_1\omega_1}\right), \alpha_{11c} = \frac{k_{12}}{k_1}, \alpha_{13c} = \frac{k_{13}}{k_1}, \alpha_{21c} = \frac{k_{21}}{k_1}, \alpha_{23c} = \frac{k_{23}}{k_1},$$
$$h_{2c} = \frac{c_2}{m_1\omega_1}, h_{12c} = \frac{c_{12}}{m_1}, \Omega_1 = \frac{\Omega_{11}}{\omega_1}, \Omega_2 = \frac{\Omega_{21}}{\omega_1}, \Omega_3 = \frac{\Omega_{31}}{\omega_1}, F_1 = \frac{F_{11}}{k_1}, F_2 = \frac{F_{21}}{k_1}, F_3 = \frac{F_{31}}{k_1}, F_{c1} = \alpha_{2c}k_c n d_{33}$$

3. Mathematical Analysis by HBM

In the present section, the HBM with slowly varying parameter is employed to analyze the steady-state dynamics of the system. To this end, assuming the solutions of Eq.. (4) and (5) as

$$x_2(\tau) = A(\tau)\cos(\Omega_i\tau + \varphi_2(\tau)) \quad (6)$$
$$x_{d1}(\tau - \tau_d) = A(\tau - \tau_d)\cos(\Omega_i(\tau - \tau_d) + \varphi_1(\tau - \tau_d)) \quad (7)$$
$$x_2(\tau) = B(\tau)\cos(\Omega_i\tau + \varphi_2(\tau)) \quad (8)$$
$$x_{d2}(\tau - \tau_d) = B(\tau - \tau_d)\cos(\Omega_i(\tau - \tau_d) + \varphi_2(\tau - \tau_d)) \quad (9)$$

where $A(\tau), B(\tau), \phi_1(\tau)$ and $\phi_2(\tau)$ are slowly-varying functions of time τ such that one can neglect the following terms: $\ddot{A}, \ddot{B}, \ddot{\varphi}_1, \ddot{\varphi}_2, \dot{A}\dot{\varphi}_1, \dot{B}\dot{\varphi}_2, \dot{\varphi}_1{}^2, \dot{\varphi}_2{}^2$. Substituting Eq. (6) to (9) into Eq. (4) and (5) and equating the co-efficient of $\sin\Omega t$ and $\cos\Omega t$ terms separately to zero, yields the following algebraic equations.

$$d_1\sin\varphi_1 + d_2\cos\varphi_1 + d_3\cos\varphi_2 + d_4\sin\varphi_2 = 0, \quad (10)$$
$$-d_1\cos\varphi_1 + d_2\sin\varphi_1 + d_3\sin\varphi_2 - d_4\cos\varphi_2 - F_1 = 0, \quad (11)$$
$$d_5\sin\varphi_1 + d_6\cos\varphi_1 + d_7\sin\varphi_2 + d_8\cos\varphi_2 = 0, \quad (12)$$
$$-d_5\cos\phi_1 + d_6\sin\phi_1 - d_7\cos\phi_2 + d_8\sin\phi_2 = 0. \quad (13)$$

where

$$d_1=\left(2\Omega_i\dot{\varphi}_1+\Omega_i^{\,2}\right)A-\omega_{n1}^{\,2}A-\left(\alpha_{1c}+\alpha_{2c}\right)A-h_{1c}\dot{A}-\alpha_{2c}\left(\begin{array}{l}A(\tau-\tau_d)\left(\sin\Omega_i\tau_d\sin\varphi_1\tau_d-\cos\Omega_i\tau_d\cos\varphi_1\tau_d\right)\\-B(\tau-\tau_d)\left(\sin\Omega_i\tau_d\sin\varphi_1\tau_d-\cos\Omega_i\tau_d\cos\varphi_1\tau_d\right)\end{array}\right)$$

$$-\frac{3}{4}\alpha_{13c}A^3-\frac{3}{4}\alpha_{23c}A^3+\alpha_{23c}AB\left(\frac{3}{4}B-\frac{3}{2}B\cos2\varphi_2+\frac{3}{2}A\cos\varphi_1\cos\varphi_2\right)+AF_3\cos\left(\Omega_3\tau\right)$$

$$-F_{c1}\left(\begin{array}{l}\left(2\Omega_i\dot{\varphi}_1+\Omega_i^{\,2}\right)A-2\dot{A}(\tau-\tau_d)\Omega_i\left(-\cos\Omega_i\tau_d\sin\varphi_1\tau_d-\sin\Omega_i\tau_d\cos\varphi_1\tau_d\right)\\+A(\tau-\tau_d)\Omega_i^{\,2}\left(\sin\Omega_i\tau_d\sin\varphi_1\tau_d-\cos\Omega_i\tau_d\cos\varphi_1\tau_d\right)+A(\tau-\tau_d)\dot{\varphi}_1\Omega_i\left(\sin\Omega_i\tau_d\sin\varphi_1\tau_d-\cos\Omega_i\tau_d\cos\varphi_1\tau_d\right)\end{array}\right)$$

$$d_2=-2\dot{A}\Omega_i+h_{1c}\left(-\Omega_iA-\dot{\varphi}_1A\right)-\alpha_{2c}\left(\begin{array}{l}A(\tau-\tau_d)\left(\sin\Omega_i\tau_d\cos\varphi_1\tau_d+\cos\Omega_i\tau_d\sin\varphi_1\tau_d\right)+\\B(\tau-\tau_d)\left(-\sin\Omega_i\tau_d\cos\varphi_1\tau_d+\cos\Omega_i\tau_d\sin\varphi_1\tau_d\right)\end{array}\right)$$

$$-F_{c1}\left(\begin{array}{l}-2\dot{A}\Omega_i-2\dot{A}(\tau-\tau_d)\Omega_i\left(-\cos\Omega_i\tau_d\cos\varphi_1\tau_d+\sin\Omega_i\tau_d\sin\varphi_1\tau_d\right)\\+A(\tau-\tau_d)\Omega_i^{\,2}\left(\sin\Omega_i\tau_d\cos\varphi_1\tau_d+\cos\Omega_i\tau_d\sin\varphi_1\tau_d\right)+A(\tau-\tau_d)\dot{\varphi}_1\Omega_i\left(\sin\Omega_i\tau_d\cos\varphi_1\tau_d+\cos\Omega_i\tau_d\sin\varphi_1\tau_d\right)\end{array}\right)$$

$$d_3=h_{2c}B\left(\Omega_i+\dot{\varphi}_2\right)$$

$$d_4=\left(\alpha_{1c}+\alpha_{2c}\right)B+\frac{3}{4}\alpha_{23c}B^3+\alpha_{23c}AB\left(\frac{3}{2}A-\frac{3}{4}A\cos2\varphi_1-\frac{3}{2}B\cos\varphi_1\cos\varphi_2\right)+h_{2c}\dot{B}$$

$$d_5=\mu\left(\alpha_{1c}+\alpha_{2c}\right)A+\mu\alpha_{2c}\left(\begin{array}{l}A(\tau-\tau_d)\sin\Omega_i\tau_d\sin\varphi_1\tau_d-A(\tau-\tau_d)\left(\cos\Omega_i\tau_d\cos\varphi_1\tau_d\right)\\-B(\tau-\tau_d)\sin\Omega_i\tau_d\sin\varphi_1\tau_d+B(\tau-\tau_d)\left(\cos\Omega_i\tau_d\cos\varphi_1\tau_d\right)\end{array}\right)+\frac{3}{4}\mu\alpha_{23c}A^3$$

$$-\mu\alpha_{23c}AB\left(\frac{3}{4}B-\frac{3}{2}B\cos2\varphi_2+\frac{3}{2}A\cos\varphi_1\cos\varphi_2\right)+\mu h_{2c}\dot{A}$$

$$-\mu F_{c1}\left(\begin{array}{l}\left(2\Omega_i\dot{\varphi}_1+\Omega_i^{\,2}\right)A-2\dot{A}(\tau-\tau_d)\Omega_i\left(-\cos\Omega_i\tau_d\sin\varphi_1\tau_d-\sin\Omega_i\tau_d\cos\varphi_1\tau_d\right)+A(\tau-\tau_d)\Omega_i^{\,2}\\\left(\sin\Omega_i\tau_d\sin\varphi_1\tau_d-\cos\Omega_i\tau_d\cos\varphi_1\tau_d\right)+A(\tau-\tau_d)\dot{\varphi}_1\Omega_i\left(+\sin\Omega_i\tau_d\sin\varphi_1\tau_d-\cos\Omega_i\tau_d\cos\varphi_1\tau_d\right)\end{array}\right)$$

$$d_6=\mu h_{2c}\left(-\Omega_iA-\dot{\varphi}_1A\right)+\mu\alpha_{2c}\left(\begin{array}{l}A(\tau-\tau_d)\left(\sin\Omega_i\tau_d\cos\varphi_1\tau_d\right)-A(\tau-\tau_d)\left(-\cos\Omega_i\tau_d\sin\varphi_1\tau_d\right)\\-B(\tau-\tau_d)\left(\sin\Omega_i\tau_d\cos\varphi_1\tau_d\right)+B(\tau-\tau_d)\left(-\cos\Omega_i\tau_d\sin\varphi_1\tau_d\right)\end{array}\right)$$

$$-\mu F_{c1}\left(\begin{array}{l}-2\dot{A}\Omega_i-2\dot{A}(\tau-\tau_d)\Omega_i\left(-\cos\Omega_i\tau_d\cos\varphi_1\tau_d+\sin\Omega_i\tau_d\sin\varphi_1\tau_d\right)\\+A(\tau-\tau_d)\Omega_i^{\,2}\left(\sin\Omega_i\tau_d\cos\varphi_1\tau_d+\cos\Omega_i\tau_d\sin\varphi_1\tau_d\right)\\+A(\tau-\tau_d)\dot{\varphi}_1\Omega_i\left(\sin\Omega_i\tau_d\cos\varphi_1\tau_d+\cos\Omega_i\tau_d\sin\varphi_1\tau_d\right)\end{array}\right)$$

$$d_7=\left(2\Omega_i\dot{\varphi}_2+\Omega_i^{\,2}\right)B-B\omega_2^{\,2}-B\mu\alpha_{2c}-\frac{3}{4}\mu\alpha_{23c}B^3-\mu\alpha_{23c}AB\left(\begin{array}{l}\frac{3}{2}A-\frac{3}{4}A\cos2\varphi_1\\-\frac{3}{2}B\cos\varphi_1\cos\varphi_2\end{array}\right)-\mu h_{2c}\dot{B}$$

$$d_8=-2\dot{B}\Omega_i+\mu h_{2c}\left(-B\Omega_i-B\dot{\varphi}_2\right)$$

Recasting Eq. (10) to (13) in the following compact matrix form:

$$\begin{bmatrix}a_1&a_2&a_3&a_4\\a_5&a_6&a_7&a_8\\a_9&a_{10}&a_{11}&a_{12}\\a_{13}&a_{14}&a_{15}&a_{16}\end{bmatrix}\begin{Bmatrix}\dot{A}\\\dot{B}\\\dot{\varphi}_1\\\dot{\varphi}_2\end{Bmatrix}=\begin{Bmatrix}b_1\\b_2\\b_3\\b_4\end{Bmatrix}\tag{14}$$

Proceedings of 61st Congress of ISTAM (http://istam.iitkgp.ac.in)
Held at: VITU - Vellore, India, Dec. 11-14, 2016 (http://www.vit.ac.in/)

From Eq. (14) the following amplitude and phase equations, also known as the slow flow equations are obtained.

$$\dot{A} = f_1(A, B, \varphi_1, \varphi_2) \tag{15}$$

$$\dot{B} = f_2(A, B, \varphi_1, \varphi_2) \tag{16}$$

$$\dot{\varphi}_1 = f_3(A, B, \varphi_1, \varphi_2) \tag{17}$$

$$\dot{\varphi}_2 = f_4(A, B, \varphi_1, \varphi_2) \tag{18}$$

The steady-state solutions of the slow-flow equations can be obtained when the first derivatives of the slowly varying amplitudes and phase are equal to zero, i.e., setting $\dot{A} = \dot{B} = \dot{\varphi}_1 = \dot{\varphi}_2 = 0$ in the Eqns. (10) to (13) one can obtain the steady-state equations as

$$p_1 \sin\varphi_1 + p_2 \cos\varphi_1 + p_3 \cos\varphi_2 + p_4 \sin\varphi_2 = 0, \tag{19}$$

$$-p_1 \cos\varphi_1 + p_2 \sin\varphi_1 + p_3 \sin\varphi_2 - p_4 \cos\varphi_2 - F_1 = 0, \tag{20}$$

$$p_5 \sin\varphi_1 + p_6 \cos\varphi_1 + p_7 \sin\varphi_2 + p_8 \cos\varphi_2 = 0, \tag{21}$$

$$-p_5 \cos\varphi_1 + p_6 \sin\varphi_1 - p_7 \cos\varphi_2 + p_8 \sin\varphi_2 = 0, \tag{22}$$

where

$$p_1 = A\begin{pmatrix} \Omega_i^2 - \omega_{n1}^2 - (\alpha_{1c} + \alpha_{2c}) - \alpha_{2c}\left(\sin\Omega_i\tau_d \sin\varphi_1\tau_d - \cos\Omega_i\tau_d \cos\varphi_1\tau_d\right) + F_3\cos(\Omega_3\tau) \\ -F_{c1}\left(\Omega_i^2 + \Omega_i^2\left(\sin\Omega_i\tau_d \sin\varphi_1\tau_d - \cos\Omega_i\tau_d \cos\varphi_1\tau_d\right)\right) \end{pmatrix} - \frac{3}{4}\alpha_{13c}A^3$$

$$-\frac{3}{4}\alpha_{23c}A^3 + \alpha_{23c}AB\left(\frac{3}{4}B - \frac{3}{2}B\cos 2\varphi_2 + \frac{3}{2}A\cos\varphi_1\cos\varphi_2\right) + \alpha_{2c}B\left(\sin\Omega_i\tau_d \sin\varphi_1\tau_d - \cos\Omega_i\tau_d \cos\varphi_1\tau_d\right)$$

$$p_2 = A\left(-h_{1c}\Omega_i - \alpha_{2c}\left(\sin\Omega_i\tau_d \cos\varphi_1\tau_d + \cos\Omega_i\tau_d \sin\varphi_1\tau_d\right) - F_{c1}\Omega_i^2\left(\sin\Omega_i\tau_d \cos\varphi_1\tau_d + \cos\Omega_i\tau_d \sin\varphi_1\tau_d\right)\right)$$
$$-\alpha_{2c}B\left(-\sin\Omega_i\tau_d \cos\varphi_1\tau_d + \cos\Omega_i\tau_d \sin\varphi_1\tau_d\right)$$

$$p_3 = h_{2c}\Omega_i B$$

$$p_4 = (\alpha_{1c} + \alpha_{2c})B + \frac{3}{4}\alpha_{23c}B^3 + \alpha_{23c}AB\left(\frac{3}{2}A - \frac{3}{4}A\cos 2\varphi_1 - \frac{3}{2}B\cos\varphi_1\cos\varphi_2\right)$$

$$p_5 = \mu A\left((\alpha_{1c} + \alpha_{2c}) + \alpha_{2c}\left(\sin\Omega_i\tau_d \sin\varphi_1\tau_d - \cos\Omega_i\tau_d \cos\varphi_1\tau_d\right) - F_{c1}\Omega_i^2\left(\sin\Omega_i\tau_d \sin\varphi_1\tau_d - \cos\Omega_i\tau_d \cos\varphi_1\tau_d\right)\right)$$
$$+\frac{3}{4}\mu\alpha_{23c}A^3 - \mu\alpha_{23c}AB\left(\frac{3}{4}B - \frac{3}{2}B\cos 2\varphi_2 + \frac{3}{2}A\cos\varphi_1\cos\varphi_2\right) - \mu\alpha_{2c}B\left(\sin\Omega_i\tau_d \sin\varphi_1\tau_d - \cos\Omega_i\tau_d \cos\varphi_1\tau_d\right)$$

$$p_6 = \mu A\left(-h_{2c}\Omega_i + \alpha_{2c}\left(\sin\Omega_i\tau_d \cos\varphi_1\tau_d + \cos\Omega_i\tau_d \sin\varphi_1\tau_d\right) - F_{c1}\Omega_i^2\left(\sin\Omega_i\tau_d \cos\varphi_1\tau_d + \cos\Omega_i\tau_d \sin\varphi_1\tau_d\right)\right)$$
$$-\mu\alpha_{2c}B\left(\sin\Omega_i\tau_d \cos\varphi_1\tau_d + \cos\Omega_i\tau_d \sin\varphi_1\tau_d\right)$$

$$p_7 = \Omega_i^2 B - B\omega_2^2 - \mu B\alpha_{2c} - \frac{3}{4}\mu\alpha_{23c}B^3 - \mu\alpha_{23c}AB\left(\frac{3}{2}A - \frac{3}{4}A\cos 2\varphi_1 - \frac{3}{2}B\cos\varphi_1\cos\varphi_2\right)$$

$$p_8 = -\mu h_{2c}B\Omega_i$$

Proceedings of 61st Congress of ISTAM (http://istam.iitkgp.ac.in)
Held at: VITU - Vellore, India, Dec. 11-14, 2016 (http://www.vit.ac.in/)

The stability of the steady-state solutions of the slow-flow equation thus obtained can be ascertained by computing the eigenvalues of the Jacobian matrix which are obtained by perturbing the Eq. (10) to (13). The stability of a particular solution is ensured by the negative real part of the eigenvalues of the Jacobian matrix.

4. Results and Discussions

In this section a parametric study is undertaken to study the effects of controlling force and stiffness α_{2c} on the frequency response characteristics. Several non-dimensional parameters involved in the problem are assumed as excitation forces $F_1 = 0.1$ and $F_3 = 0.01$, mass ratio μ=100, damping's in both the primary and the absorber are considered to be $h_{1c} = 0.002, h_{2c} = 0.0004$ and the stiffness α_{2c} value varied from 0.001 to 1. The quadratic and cubic nonlinearity stiffness is considered to be 3% and 4% of the linear stiffness for the primary system and the absorber respectively. The value of F_{c1} is obtained by considering number of wafers n in the PZT actuator equal to 100 and stiffness of the PZT actuator is referred from [5]. The control gain k_c is varied from 1 to 100 to provide an actuating force by the PZT actuator from 0 to 0.002.

In the Fig.2 time responses of both the primary system and the absorber are studied at non resonant frequency region by numerical method using MATLAB command *dde23* for the Eq. (4) and Eq. (5). From the Fig. 2(a), it can be observed that by applying controlling force the settling time is very less than for the system without controlling force. In Fig. 2(b) the effect α_{2c} on both primary system and absorber is studied and it is compared with Fig. 2(c) where by increasing the α_{2c} the amplitude of both the primary system and the absorber is decreased. The maximum amplitude at steady state in the Fig 2(b) for absorber is 1.02 and for primary system it is 0.36. However in Fig. 2(c) maximum amplitude at steady state in the Fig 2(c) for absorber is 0.006 and for primary system it is 0.01.

In Fig 3. time responses of the primary system and the absorber are studied at resonant frequency, i.e. when $\Omega_i = 1$ and $\Omega_3 = 0.9$. The amplitude of both primary system and absorber are higher compared to those Fig. 2. The effects of time delay on the response are compared using MATLAB command *dde23* (Fig. 3 (a), (b)) and of MATLAB command *ode45* (Fig. 3 (c), (d)) for the system with and without delay respectively. It is observed that time delay in the limit from 0.1 to 0.8 gives better vibration suppression than without no delay. From the Fig. 3(a) the amplitude of primary system with a delay of 0.5 is 0.42 and for the system with no delay the amplitude is found to be 2.2 (Fig. 3(c)). The same observations are also detected in case of the absorber as shown in Fig. 3 (b) and 3(d). For a delay of 0.5 the response amplitude of the absorber is found to be 2.8 and when there is no delay the response amplitude is 5.2.

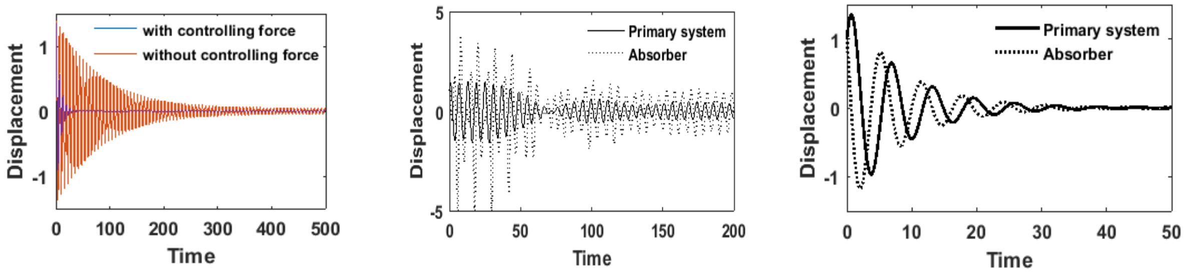

Fig.2. Time domain response of (a) primary system by with $F_{c1} = 0$ and $F_{c1} = 0.002$ (b) primary system and absorber with $F_{c1} = 0.002$ and $\alpha_{2c} = 0.001$ (c) primary system and absorber with $F_{c1} = 0.002$ and $\alpha_{2c} = 0.1$.

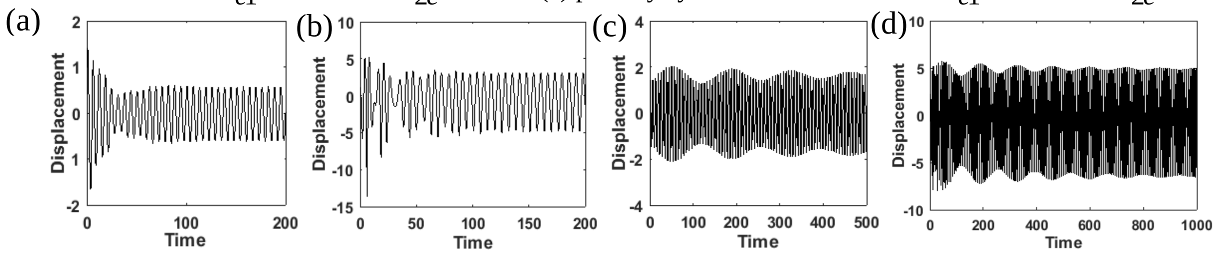

Fig.3. Time domain response with $F_{c1} = 0.002$ and $\alpha_{2c} = 0.001$ (a) primary system with time delay and (b) absorber with time delay and (c) primary system with no delay and (d) absorber with no delay

Hence by using a delay of 0.5 the amplitude of primary system is reduced by 81% and the response amplitude of the absorber is reduced by 47%. The frequency response plots of the primary system and the absorber are obtained by solving Eq. (19) to (22) using Newton Raphson method. The frequency response of the primary system with the controlling force is shown in the Fig. 4(a) with applied controlling force. It is observed from the Fig. 4 (a) that the maximum amplitude of the primary system is equal to 0.36 at the frequency of 0.92 after which the amplitude reduces. The instability region in the frequency response of the primary system also observed in the range

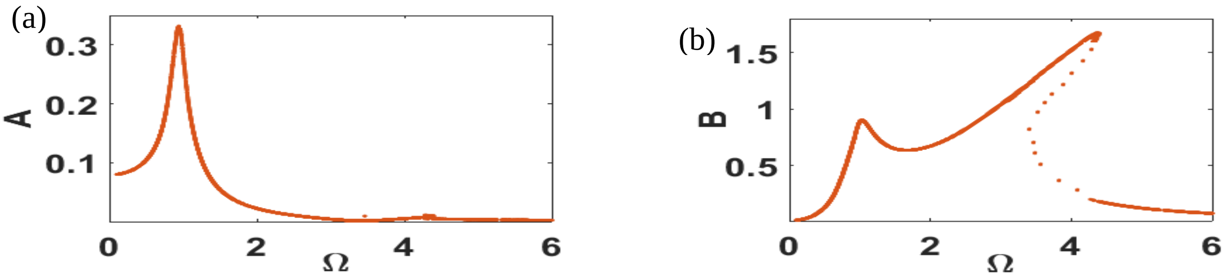

Fig.4. Frequency response plot with $F_{c1} = 0.002$ and $\alpha_{2c} = 0.001$ (a) primary system (b) absorber

4.2 to 4.4. In the Fig. 4 (b) the frequency response of the absorber is plotted from which one can observe two high peaks of 1.04 and 1.64 at frequency operation of 0.88 and 1.62, respectively. The amplitude responses between the two peaks are of different value this can be minimized by obtaining optimized value for the damping in the absorber and stiffness in the absorber. The nonlinearity effect in the absorber also observed which bends the frequency response curve in the range of 2.1 to 4.2. The frequency response of the primary system and the absorber with controlling but without delay is plotted in the Fig. 5. In the Fig. 5(a) the maximum amplitude of the primary system is 1 at a frequency of 0.72 which is comparatively higher than the response obtained in the

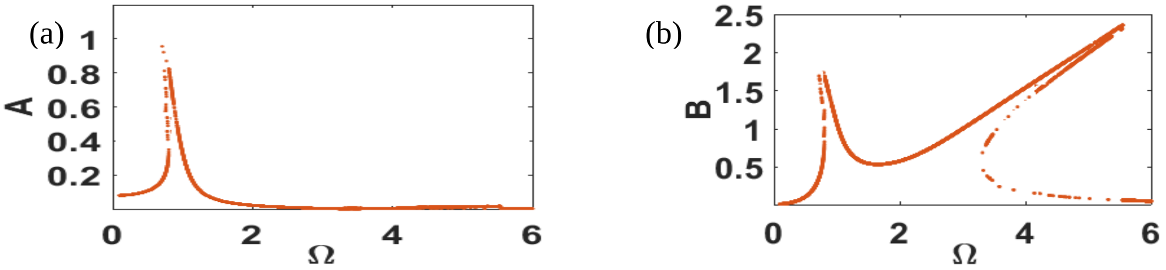

Fig.5. Frequency response plot with no delay (a) primary system (b) absorber.

Fig 4(a). From Fig. 5(b) it is observed that the amplitude of the absorber has two peaks of 1.8 and 2.32 at the frequency 0.7 and 5.6 respectively. The frequency response of the primary system and absorber without applied controlling force is shown in the Fig. 6. The maximum amplitude of primary system and the absorber are 4.2 and 3.8 at frequency of operation 0.82 and 0.86 respectively. In the Fig. 6(b) the responses of the primary system and the absorber is shown without the applied controlling force. The amplitude response of the primary system in the Fig 6(a) is found

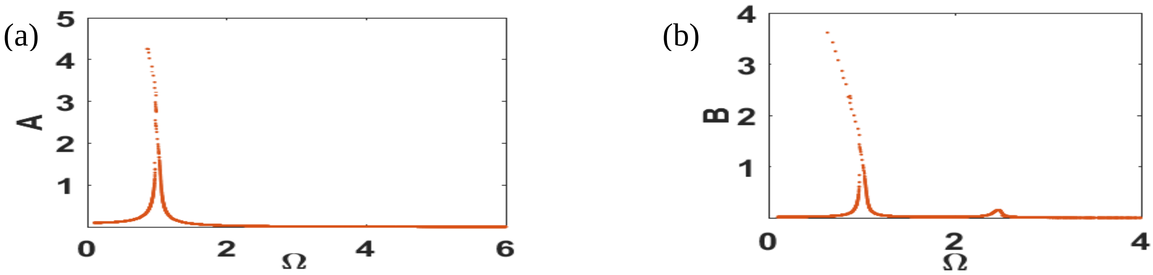

Fig.6. Frequency response plot with no controlling force (a) primary system (b) absorber.

to be 4.2 and for the absorber it is 3.8 as shown in Fig. 6(b). The frequency response plot obtained using HBM are compared with the time responses curve obtained by numeric method, which are observed that are in good agreement with each other in terms of the amplitude of the primary system and the absorber at the resonant frequency of operation.

5. Conclusions

In the present paper nonlinear hybrid vibration absorber with time delayed acceleration feedback is investigated by considering a DVA in tandem with a PZT actuator. HBM is used to obtain the frequency responses of the system and then the results are compared with those obtained using the numeric method. The response amplitude of the primary mass and the absorber are shown to be suppressed with the proper application of controlling force. The time delay in the range of 0.1 to 0.8 with acceleration feedback shows the effectiveness in attenuating the vibration of the system for the primary resonance condition. The damping ratio used in the primary system and the absorber is considered to be 0.001 and 0.0002 to shows the effectiveness of vibration suppression by the use PZT actuator. DVAs are generally designed based on the assumption that the absorber structure possesses linear characteristics. However, an effective vibration absorber vibrates with large amplitude leading to the dominance of structural nonlinearity for which here nonlinearity in the stiffness is considered. Thus, the linearity assumption regarding the elastic properties of the absorber substructure does not hold well in reality. In the proposed model as a spring of stiffness k_3 is used in series with the actuator so one can increase the controlling force without increase in the supplied voltage to the actuator. So the proposed model is more economical and also a failsafe design as when the control is on it performs better than a passive DVA and in the event of failure of active part the passive DVA can still protect the system from being damaged due to severe vibration.

References:

1. M. G Soto, and H. Adeli, Tuned mass dampers, Archives of Computational Methods in Engineering 20.4 (2013): 419-431.
2. S. Chun, Y. Lee and T. H. Kim, H∞ optimization of dynamic vibration absorber variant for vibration control of damped linear systems, Journal of Sound and Vibration 335 (2015): 55-65.
3. S. Mohanty and S. K. Dwivedy, Linear and nonlinear analysis of piezoelectric based vibration absorber with acceleration feedback, Procedia Engineering 144 (2016): 584-591.
4. J. C. Ji, Design of a nonlinear vibration absorber using three-to-one internal resonances, Mechanical Systems and Signal Processing 42.1 (2014): 236-246.
5. A. K. Mallik and S. Chatterjee, Principles of passive and active vibration control, East West Press (2014).